Development 130, 1771-1781

doi:10.1242/dev.00404

The bHLH protein Dimmed controls neuroendocrine cell differentiation in *Drosophila*

Randall S. Hewes[1,2,*], Dongkook Park[1], Sebastien A. Gauthier[2], Anneliese M. Schaefer[1] and Paul H. Taghert[1,†]

[1]Department of Anatomy and Neurobiology, Washington University School of Medicine, Saint Louis, MO 63110, USA
[2]Department of Zoology, University of Oklahoma, Norman, OK 73019, USA
*Present address: Department of Zoology, University of Oklahoma, 730 Van Vleet Oval, Norman, OK 73019, USA
†Author for correspondence (e-mail: taghertp@pcg.wustl.edu)

Accepted 9 January 2003

SUMMARY

Neuroendocrine cells are specialized to produce, maintain and release large stores of secretory peptides. We show that the *Drosophila dimmed/Mist1* bHLH gene confers such a pro-secretory phenotype on neuroendocrine cells. *dimmed* is expressed selectively in central and peripheral neuroendocrine cells. In *dimmed* mutants, these cells survive, and adopt normal cell fates and morphology. However, they display greatly diminished levels of secretory peptide mRNAs, and of diverse peptides and proteins destined for regulated secretion. Secretory peptide levels are lowered even in the presence of artificially high secretory peptide mRNA levels. In addition, overexpression of *dimmed* in a wild-type background produces a complimentary phenotype: an increase in secretory peptide levels by neuroendocrine cells, and an increase in the number of cells displaying a neuroendocrine phenotype. We propose that *dimmed* encodes an integral component of a novel mechanism by which diverse neuroendocrine lineages differentiate and maintain the pro-secretory state.

Supplemental data available online

Key words: Neuroendocrine, *Drosophila*, bHLH, Neuropeptide, Differentiation, Regulated secretion

INTRODUCTION

The differentiation of a neuroendocrine phenotype involves the selection and production of a specific peptide hormone. For both endocrine and neuroendocrine cells, recent genetic analyses in mice have revealed transcriptional hierarchies controlling such developmental events. The process typically involves multiple stages of gene activation and extinction, and it represents the actions of multiple regulatory cascades. For example, the proliferation and specification of hypothalamic neurosecretory neurons that produce vasopressin, oxytocin and corticotrophin-releasing factor are controlled by early expression of *Orthopedia* (Acampora et al., 1999) and *Sim1* (Michaud et al., 1998). These effects are mediated largely by induction or maintenance of a secondary factor, *Brn2*, which directly regulates neuropeptide gene expression (Schonemann et al., 1995; Nakai et al., 1995). Likewise, in pituitary and in pancreatic endocrine cells, tissue-specific (e.g. Ptx1/2) and secondary cell type-specific transcription factors (e.g. neurogenin3) promote patterned expression of peptide hormones (Sheng and Westphal, 1999).

Neuroendocrine cell differentiation also involves the integrated assembly of cellular machinery needed to produce large amounts of secretory peptides. Such mechanisms coordinate several events associated with the regulated secretory pathway (Arvan and Castle, 1998): the ability to synthesize, process, sort, traffic and accumulate dense-core secretory granules and their contents. Neurons differ greatly and reproducibly in the amount of secretory peptides that they produce, and in their elaboration of the secretory pathway. For example, mammalian motoneurons produce low levels of neuropeptides such CGRP or galanin (Streit et al., 1989), and at the ultrastructural level, their terminals contain many small, clear vesicles, but very few large, dense-core (peptide-containing) granules (Hall and Sanes, 1993). By contrast, hypothalamic neurosecretory neurons produce large amounts of vasopressin, oxytocin, or corticotrophin-releasing factor, and they contain correspondingly large numbers of dense-core secretory granules (Burbach et al., 2001). Cells also transiently modify their levels of secretory activity following injury (e.g. Blake-Bruzzini et al., 1997) or stimulation (e.g. Herman et al., 1991). The mechanisms underlying these differences in levels of secretory activity are unknown.

Because the amplified expression of the secretory pathway is a stable and cell-specific feature of neuroendocrine cells, we hypothesize the existence of genetic factors that control this phenotype. Identifying such factors will facilitate a detailed, mechanistic analysis of neuroendocrine cell organization and physiology. Such an analysis will be crucial to a general understanding of neuroendocrine cell biology and will support efforts to produce a program of neuroendocrine differentiation from stem cells in vitro. We describe a *Drosophila* bHLH gene,

dimmed (*dimm*), with an expression pattern that corresponds precisely to the neuronal and endocrine cells that accumulate large amounts of secretory peptides. We present both loss-of-function and gain-of-function analyses to argue that *dimm* confers a pro-secretory phenotype within these diverse cells, and that its actions appear confined to that aspect of cellular differentiation. Thus, we propose a novel and general mechanism, of which *dimm* is an essential component, for the amplification of the regulated secretory pathway by dedicated secretory cells.

MATERIALS AND METHODS

Strains

Flies were cultured at 22-25°C on a standard cornmeal-yeast-agar medium. The molecular and genetic characterization of *c929*, *R6* and *Rev8* has been described previously (Hewes et al., 2000). *Rev4* and *Rev18* are X-ray revertants of *P{PZ}l(2)k05106*^{06311} (M. Horner and C. Thummel, personal communication). y^{-} w^{-} revertants of *KG02598* (e.g. *dimm*^{S2a}) were obtained by transposase-mediated excision, and each line was characterized by PCR with primers flanking the original insertion site. Except as noted, all other strains are described elsewhere (Lindsley and Zimm, 1992; FlyBase, 1999) and were obtained from the Bloomington stock center, the BDGP Gene Disruption Project and other sources.

Scoring of *dimm* larvae

Eggs were collected on apple juice-agar plates supplemented with yeast paste. Larvae were collected from the plates, and heterozygotes (y^{*} w^{*} and balanced over *CyO-y*$^{+}$) were distinguished by mouthpart color. After scoring, size-matched pairs of y^{-} and y^{+} larvae were dissected and stained in parallel.

Immunostaining

Immunostaining was performed as described previously (Benveniste et al., 1998). Briefly, tissues were fixed in 4% paraformaldehyde (PFA), Bouin's, or 4% paraformaldehyde/7% picric acid (PFA-PA). Polyclonal or monoclonal primary antisera were used (overnight at 4°C) to detect the following proteins: β-gal (1:1000, PFA-PA; Promega); PHM (1:750 pre-absorbed to PHM$^{-/-}$ larvae, Bouin's) (Jiang et al., 2000); -RFa ('PT2')(1:2000, PFA-PA) (Taghert, 1999); FMRF (1:2000, PFA-PA) (Chin et al., 1990); corazonin (1:500, Texas Red-conjugated; PFA-PA) (Veenstra, 1994); LK (1:500, PFA-PA) (Nässel and Lundquist, 1991); CCAP (1:400, PFA-PA) (Ewer and Truman, 1996); PDH and PAP (each 1:2000, PFA-PA) (Renn et al., 1999); MM (1:800, PFA-PA) (O'Brien and Taghert, 1998); dopa decarboxylase (affinity purified 1:100, PFA) (Scholnick et al., 1991); Furin-1 (1:1000, Bouin's) (Jiang et al., 2000); and Myc (1:500, PFA-PA; a gift from Y.-N. Jan; Sigma). Secondaries used were goat Cy3, FITC, Texas Red or ALEXA 488 conjugates (Jackson ImmunoResearch) at a 1:500 dilution. Confocal *z*-series projections were obtained using an Olympus Fluoview microscope.

RACE

A cDNA library was made from RNA of *y w* adult heads using commercial reagents (Clontech). 5′ RACE was performed according to manufacturer's recommendations using *CG8667*-specific primers.

dimm RNAi

RNAi was performed based on the methods of Kennerdell and Carthew (Kennerdell and Carthew, 1998) and Clemens et al. (Clemens et al., 2000). The template for RNA synthesis was generated by PCR, using primers containing a T7 promoter sequence (5′-GAATTA-ATACGACTCACTATAGGGAGA-3′) at the 5′ ends and P1 DNA (DS00532) as the PCR template. The gene specific primers 5′-CAGATTCCAGTTCGCAAAGCGAT-3′ and 5′-GGGCTCGTCG-AAATTATCATTGATA-3′ amplified a 951 bp segment of open reading frame in exon 3, including the entire bHLH domain. Transcription and analysis of the double-stranded RNA (dsRNA) were performed as described (Clemens et al., 2000). dsRNA (3 μM) was injected into syncytial blastoderm embryos (Canton-S) ~75% along the anteroposterior axis. For the mock controls, all steps were performed in parallel, except that the P1 DNA was omitted from the PCR reaction. Mock- and RNA-injected larvae were dissected during or within 6 hours after hatching.

UAS-dimm transgene

The predicted coding region of *CG8667* was amplified by PCR using cDNA generated from *y w* adult head RNA (Clontech). The primers 5′-CAGATCTCGACGATTTTTGTTCAGCCAT-3′ (5′ UTR) and 5′-TGCGGCCGCAGAAACTCTCGAAAGGGCT-3′ (end of the ORF) were used to construct a 1236 bp fragment that was cloned into *pBSK+* and then transferred to *pP{UAST-Myc}* at the *Bgl*II and *Not*I sites. Transgenic lines containing *P{UAS-dimm::Myc}* insertions were created using standard techniques (Benveniste and Taghert, 1999). *UAS-dimm::Myc*$^{2\text{-}A\text{-}3}$, *Rev8/CyO, Act-GFP* flies were crossed to *c127-Gal4, UAS-GFP*; *Rev4/CyO, Act-GFP*, and first instar larvae were scored for *Act-GFP*- and *c127*-specific GFP labeling patterns.

mRNA in situ hybridization

Whole-mount in situ hybridization (Tautz and Pfeifle, 1989) was performed using single-stranded, digoxigenin-labeled RNA or DNA probes (Patel, 1996) prepared from P1 or cDNA templates.

Staining quantification

Cells were imaged on a Zeiss Axioplan fitted with a SPOT CCD camera and software (Diagnostic Instruments) or in confocal *z*-series scans. Exposure settings were adjusted to optimize detection without saturating the signal. For a given neuron, identical settings were used for all preparations and genotypes. Mean pixel luminosity for the area covering the soma (S) was measured for each neuron using Adobe Photoshop. An adjacent area was sampled to measure the background signal (B). The intensity index=(S–B)/B. Cells not visible were scored 0. Cells that were obscured or lost due to tissue damage were not analyzed. Brightfield images were inverted before quantification. CNS size was measured as an additional control – in each case, mean brain lobe diameters were not significantly different between genotypes (data not shown). Statistics were performed using the NCSS-2000 Statistical Analysis System or StatView (MANOVAs; Games-Howell). Variances are reported as ±s.e.m.

RESULTS

c929 is broadly expressed in peptidergic cells

The *c929 P*-element insertion was isolated in a *P{Gal4}* enhancer detection screen for genes expressed in the Tv neuroendocrine neurons (O'Brien and Taghert, 1998). In addition to the Tv neurons, *c929* drove reporter gene expression (GFP or β-galactosidase) in ~200 neurons scattered throughout the larval CNS and in neuroendocrine projections to the ring gland, the dorsal neurohemal organs and the transverse nerves (Fig. 1A). Outside the CNS, this pattern included at least three classes of endocrine cells: intrinsic cells of the corpora cardiaca (Fig. 1A), 10-20 midgut cells (data not shown) and the peritracheal myomodulin-immunoreactive cells. The latter appear homologous to the endocrine Inka cells (O'Brien and Taghert, 1998). *c929* reporter expression also appeared in several other tissues, including peptidergic PNS neurons (LBD neurons; D. Allan and S. Thor, personal

communication), fat body, epithelial cells and salivary glands (data not shown).

To determine whether *c929*-positive neurons express neuropeptides, we performed double-label experiments for the *c929* reporter and for the peptide biosynthetic enzyme, peptidylglycine-α-hydroxylating monooxygenase (PHM). In *Drosophila*, PHM is a marker for most peptidergic cells. It is required for neuropeptide amidation (Jiang et al., 2000), which is a highly specific modification of secretory peptides (Eipper et al., 1993); greater than 90% of all known or predicted *Drosophila* peptide transmitters are amidated (Hewes and Taghert, 2001). Most if not all *c929*-positive CNS neurons were immunostained very strongly by PHM antibodies (*n*=8 specimens; Fig. 1B,E).

Conversely, most neurons displaying strong PHM immunostaining were also *c929* positive, while most weakly PHM-positive neurons were not *c929* positive (data not shown). In addition, PHM was expressed in all three *c929*-positive endocrine cell types and in the LBD peripheral neurons (O'Brien and Taghert, 1998) (data not shown). Thus, in the larval CNS and in several peripheral tissues, *c929* primarily labels neuroendocrine cells as its expression was highly correlated with the production of large amounts of amidating enzyme, amidated neuropeptides and peptide hormones.

To assess the degree of heterogeneity among *c929*-positive cells, we compared the expression pattern of *c929* with a variety of other peptidergic cell markers. This population of cells was chemically diverse. For example, seven bilateral pairs of *c929*-positive neurons were double-labeled with the PT2 antiserum (Fig. 1C,E). PT2 is a marker for -RFamide containing neuropeptides, which include the products of at least three *Drosophila* genes (Taghert, 1999). Additional subsets of *c929*-positive neurons were immunostained with antisera directed against a variety of neuropeptides. These included the *Drosophila* FMRF propeptide (*n*=8 specimens), cockroach corazonin (*n*=5), cricket leucokinin-1 (LK), crustacean cardioactive peptide (CCAP; *n*=4), crustacean beta-PDH (*n*=4) and *Aplysia* myomodulin (MM; Fig. 1D,E). Finally, a distinct subset of 34 *c929*-positive neurons (see below) was immunopositive for an additional, putative *Drosophila* peptide biosynthetic enzyme (*n*=10; P.H.T. and M. Han, unpublished) Furin 1 (De Bie et al., 1995). Based on their positions, cellular morphologies, and immunostaining with the above markers, the cells within the *c929* pattern represent more than 26 distinct classes of peptidergic neurons and endocrine cells. No *c929*-positive neurons were stained with an antiserum to dopa decarboxylase (*n*=8), an enzyme required for synthesis of the biogenic amines, serotonin and dopamine (Hirsh, 1989).

No single transmitter system we tested was entirely *c929* positive. For example, among the

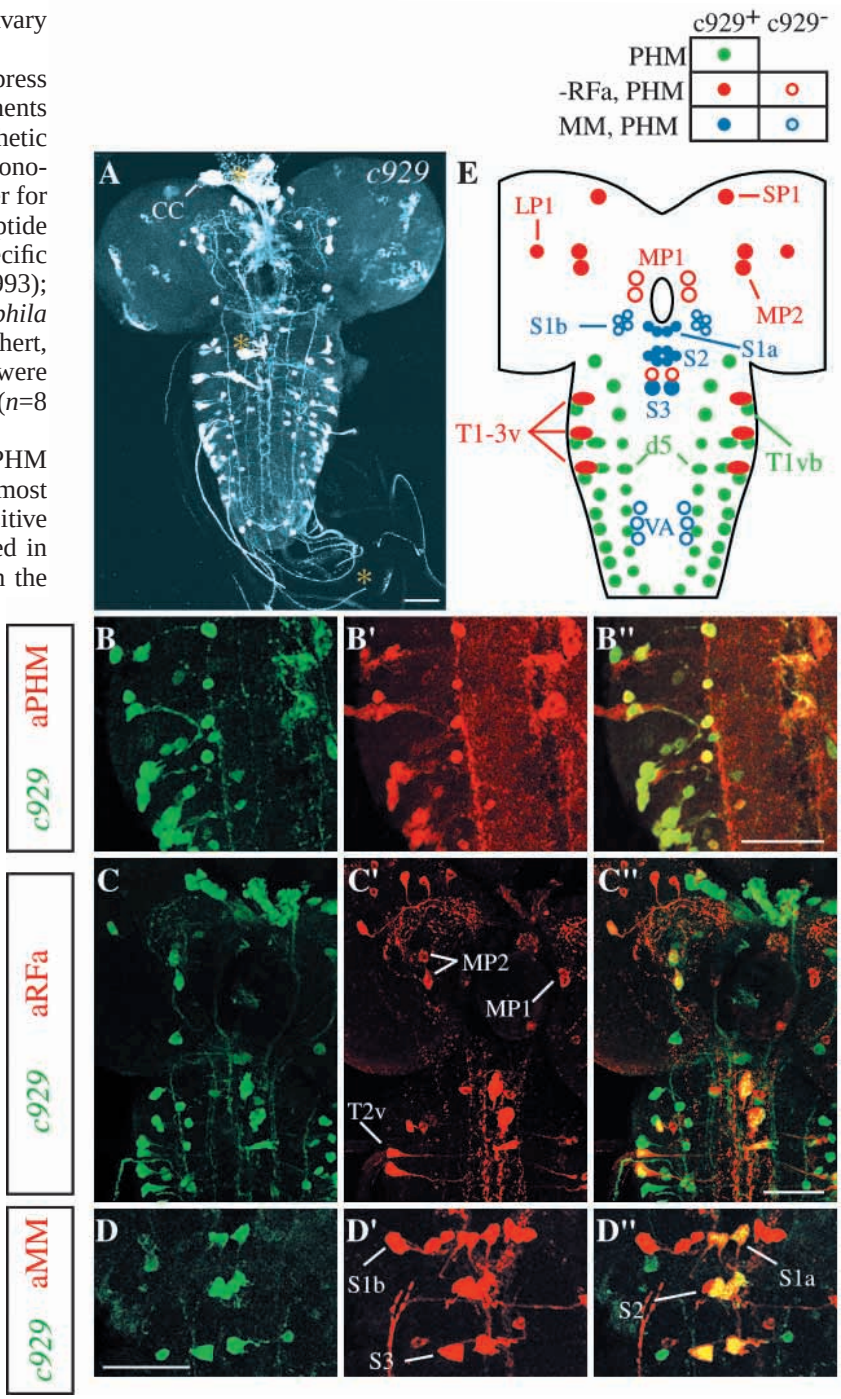

Fig. 1. The *c929* reporter gene is expressed in ~200 peptidergic CNS neurons. (A) Confocal *z*-series of *c929* reporter (*c929-Gal4,* P{*UAS-lacZ*}Bg4-1-2) expression in the larval CNS. Expression is detected in ~200 neurons, in neuroendocrine release sites (asterisks) and in intrinsic cells of the endocrine corpora cardiaca (CC) (*n*>50). (B,B′) Double-labeling for *c929* reporter (B) and the peptide biosynthetic enzyme, PHM (B′). Yellow cells in the overlay (B″) were positive for both markers (*n*=8). (C) Double-labeling (C″) for *c929* reporter (C; *P{UAS-GFP}D1*) (Yeh et al., 1995) and neuropeptides ending in the epitope, RF-amide (PT2 antiserum; αRFa, C′) (*n*=10). (D) Double-labeling (D″) for *c929* reporter (D) and neuropeptides related to MM (D′) (*n*=10). (E) Schematic illustration of the expression patterns for the *c929* reporter, the PHM enzyme, and MM- or RFa-immunoreactive neuropeptides. Although generally *c929* negative at this stage (mid-third larval instar), the MP1 and VA neurons express the *c929* reporter gene for one or more brief periods during development. Scale bars: 50 μm.

17 *Fmrf* cell types (Benveniste and Taghert, 1999), only the Tv neurons were *c929*-positive. However, in third instar larvae there were some *c929*-negative neurons, such as the peptidergic MP1s and VAs, which displayed weak and/or transient *c929* reporter expression during other stages of development (e.g. Fig. 5G). Thus, our identification of *c929*-positive peptidergic neurons is likely to be an underestimate of the total population of peptidergic cells that express the reporter gene.

dimm is required for maintenance of neurosecretory protein levels

To test for roles of a putative '*c929*' gene in the development and/or function of peptidergic cells, we generated deletions flanking the *c929* insertion site (Fig. 2A). These deletions caused recessive lethality, owing to disruption of at least one essential gene, *cryptocephal* (*crc*) (Hewes et al., 2000). However, many homozygous mutant animals survived into the larval stages, when we could examine the fates of CNS peptidergic neurons.

By immunostaining the mutant animals for PHM, we detected a novel phenotype: *R6/Rev8* trans-heterozygous animals contain small deficiencies around the *c929* insertion site that are ~12 and ~ 35 kb respectively (Fig. 2A). Trans-heterozygous larvae displayed marked reductions in PHM protein levels in all strongly *c929*-positive CNS neurons (Fig. 2B). *c929*-negative neurons were unaffected in *R6/Rev8* larvae, and weakly or transiently *c929*-positive neurons, such as the VAs, showed smaller reductions in PHM immunostaining (Fig. 2B). The mutant phenotype was detectable at the time of larval hatching and throughout all larval stages. By contrast, heterozygous *R6* or *Rev8*/+ larvae were essentially wild type, although these alleles displayed mild haploinsufficiency (n=24; data not shown) with other markers (see below). These results demonstrate a requirement for ~10 kb of DNA flanking the *c929* insertion site for the normal expression and/or maintenance of PHM in *c929*-positive CNS neurons. We named the affected gene *dimmed* to reflect the diminished staining.

We used six additional neurosecretory markers in *dimm* mutant larvae, and found that all six displayed moderate to severe reductions in immunostaining in spatial patterns corresponding to the *c929* reporter pattern. The affected proteins included several known or presumed neuropeptides – MM (Fig. 2C), LK (n>25), the FMRF propeptide (n>12) and several PT2 positive neuropeptides (n>50) – and the putative neuropeptide biosynthetic enzyme Furin 1 (see below). All *c929*-positive neurons displayed the mutant phenotype for at least one marker, PHM (Fig. 2B); many showed reduced immunostaining with multiple markers. For example, the Tv neurons had reduced

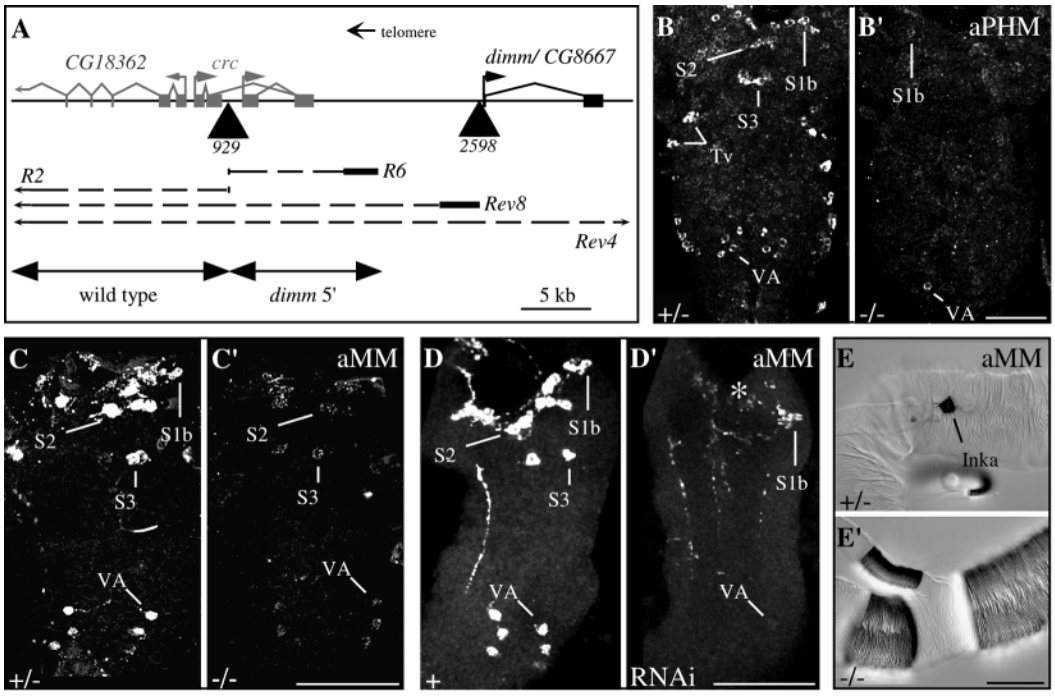

Fig. 2. *dimm* is required for expression of normal levels of peptide transmitters. (A) The 39C4-D1 region of chromosome 2L showing the locations of the *c929* and *KG02598* ('*2598*') *P* element insertions (triangles), the *CG18362*, *cryptocephal* (*crc*) and *dimm* (*CG8667*, *Mistr*) genes, and local deletions (wavy lines; bars indicate breakpoint uncertainties). *TW1* (not shown) deletes 38A7-B1 to 39C3, ending ~17 kb distal to the *c929* insertion (Hewes et al., 2000). *Rev18* deletes chromosomal bands 39A3-7 to 39D3-5 (A. Carpenter, personal communication). *Rev4* deletes 39C1-4 (Hewes et al., 2000) and is a molecular null for the *dimm* gene (D. Eberl, personal communication; data not shown). Introns smaller than 70 bp are not shown. A segment of DNA extending toward the telomere (wild type) was deleted without affecting neuropeptide levels in the CNS. A second region (*dimm* 5′) was required for the maintenance of normal neuropeptide levels and probably contains *dimm* 5′ enhancer elements. (B) The *dimm* mutant phenotype for a peptide biosynthetic enzyme, PHM. Reduction in PHM immunostaining in the CNS of a third instar $dimm^{-/-}$ larva (B′), compared with a $dimm^{+/-}$ sibling control (B) (n=28).(C) The *dimm* mutant phenotype for neuropeptides related to MM. Reduction in MM immunostaining in the CNS of a first instar $dimm^{-/-}$ larva (C′), compared with a $dimm^{+/-}$ sibling control (C) (n>50). (D) Phenocopy of the $dimm^{-/-}$ phenotype (MM immunostaining) by injection of double-stranded *CG8667* RNA into wild-type embryos (D′), compared with a mock (saline-injected) control (D) (n=7). Asterisk, weak signal in midline S2 and/or S1a neurons. (E,E′) The *dimm* mutant phenotype in the endocrine Inka cells. Anti-MM immunostaining of an Inka cell in a third instar $dimm^{-/+}$ larva Inka cell immunostaining [E; compare with O'Brien and Taghert (O'Brien and Taghert, 1998)] was no longer detectable in a $dimm^{-/-}$ larva (E′). The apparent increase in background in E′ is due to the incidence of air pockets in the tracheae of this specimen. The precise location of the Inka cell is variable and not certain in (E′); however, it is normally within this image field. Scale bars: 50 μm.

levels of PHM, the FMRF propeptide, –RFamide peptides and Furin 1 (Fig. 2B, see Fig. 3B, see Fig. 6B). Thus, in a large and diverse population of CNS peptidergic neurons, *dimm* regulates levels of a broad array of secretory proteins.

As the three classes of *c929*-positive endocrine cells also likely secrete peptide hormones, we also tested them for effects of the *dimm* mutations. The ring gland (n=15) and tracheal endocrine cells (n>50) displayed severe reductions in peptide immunostaining for PHM and/or MM in $dimm^{-/-}$ mutants (Fig. 2E; data not shown); the gut endocrine cells were not tested. Taken together, these results suggest a crucial role for *dimm* in controlling bioactive peptide levels in diverse neuronal and endocrine secretory cells.

dimm encodes a basic helix-loop-helix protein

Using chromosomal deletions, we genetically mapped the *dimm* gene. We performed peptide immunostaining on *Rev8* homozygotes (n=15) and on hemizygotes (n>50) bearing one copy of *R6* (or *Rev8*) over one of several independently derived deficiencies of the entire 39C4-D1 region of chromosome 2L (e.g. *Rev4*). In each case, the effects on peptide immunostaining were comparable, although the reduction in MM staining in larvae homozygous for *Rev4*, a null allele (Fig. 2A), was more pronounced than in *R6/Rev8* trans-heterozygotes (n=12; data not shown). Thus, *R6* and *Rev8* are hypomorphic alleles. Normal peptide immunostaining was restored in male *Rev8* homozygotes (n=6) bearing a duplication of chromosome bands 35A-40 [*Tp(2;Y)J54*], consistent with the location of *dimm* in 39C4-D1.

In contrast to *R6/Rev8* mutants, larvae with disruptions in the *crc* gene (*c929* homozygotes, n=6; crc^{1}/*R6* trans-heterozygotes, n>40; *R2* homozygotes, n=5), or deletions of DNA extending up to 200-300 kb towards the telomere (*TW1/Rev18* trans-heterozygotes, n=7) displayed wild-type neuropeptide levels (see Table S1 at http://dev.biologists.org/supplemental/). Thus, *dimm* is not *crc*, nor is it any other gene located distal to the site of the *c929* insertion.

The closest gene proximal to *c929* is *CG8667* (*Mistr*), found within 25 kb (Fig. 2A). It encodes a basic helix-loop-helix (bHLH) protein that is a member of the Atonal subfamily of transcription factors (Moore et al., 2000). Its bHLH domain displays 79% identity with the mouse Mist1 protein (Pin et al., 1999). In *Rev8* homozygous embryos, *CG8667* mRNA expression was markedly reduced, but not eliminated (n>50; data not shown), consistent with the identification of *Rev8* as a hypomorphic *dimm* allele. After 5′ RACE identification of the 5′ end of *CG8667*, we identified a *P*-element insertion ($dimm^{KG02598}$) located 111 bp upstream (Fig. 2A). $dimm^{KG02598}$ displays homozygous lethality (see Table S2 at http://dev.biologists.org/supplemental/), and represents a severe hypomorphic *dimm* allele, because *CG8667* mRNA expression appeared low or undetectable in $dimm^{KG02598}$ *homozygous* mutant embryos (Fig. 3A). Hatchling $dimm^{KG02598}$/*Rev4* larvae displayed reduced immunostaining for PT2-positive neuropeptides (n>15; Fig. 3B). Normal PT2 immunostaining was restored (n>15; Fig. 3B) after precise excision of the $dimm^{KG02598}$ *P* element. Consistent with the conclusion that *dimm* and *crc* are separate genes, *KG02598* was

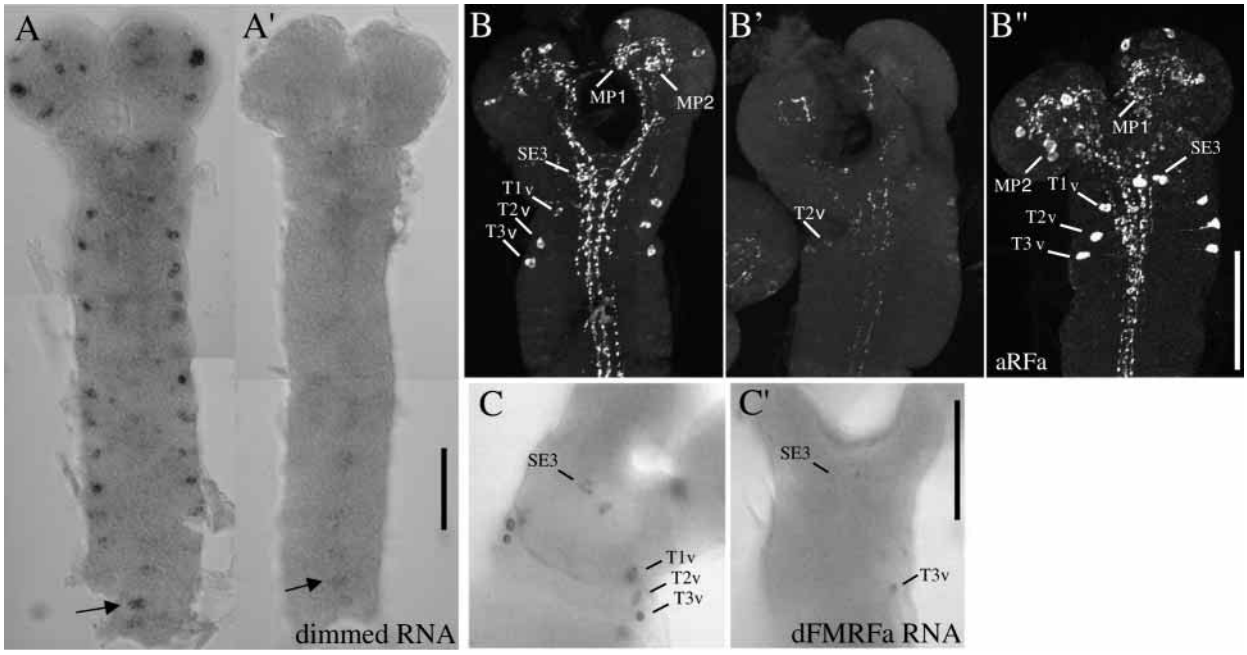

Fig. 3. The *KG02598 P*-element insertion reduces *CG8667* expression and is a strong *dimm* mutant allele. (A) Photomontages of *CG8667* in situ hybridization in homozygous stage 16 and 17 embryonic CNS: normal staining levels were observed in 7/15 specimens from the stock $dimm^{KG02598}/CyO\text{-}y^{+}$ (left); reduced staining levels were observed in the remaining eight specimens (right). In the presumed homozygotes, residual staining was seen only in unpaired cell bodies in caudal abdominal neuromeres that normally stain strongly (arrow). Normal staining levels were also found in 15 out of 15 comparable specimens from the cross $dimm^{KG02598}/CyO\text{-}y^{+}$ × *Canton S* (not shown). (B) Reduction in immunostaining with the PT2 antiserum in the CNS of a first instar $dimm^{KG02598}$/*Rev4* larva (B′), compared with a $dimm^{+/-}$ sibling control (B) and a $dimm^{S2a}$/*Rev4* control (B″). $dimm^{S2a}$ is a precise excision of the *KG02598 P*-element. (C). Photomontages of reduced *Fmrf* in situ hybridization in the CNS of a first instar $dimm^{KG02598}$/*Rev4* larva (C′) compared with a $dimm^{+/-}$ sibling control (C). Scale bars: 50 μm.

lethal when trans-heterozygous with *Rev4*, but not with *crc*^{1} (see Table S2 at http://dev.biologists.org/supplemental/). The *dimm*^{KG02598} mutation also reduces levels of secretory peptide mRNAs in the Tv neuroendocrine cells, which display high levels of *Fmrf* mRNA expression (Schneider et al., 1993): when assessed using in situ hybridization, the mean number of *Fmrf*-positive Tv neurons per CNS was 5.57 in *dimm* heterozygotes (n=7; Fig. 3C) and 2.33 in *dimm* hemizygotes (n=9; Fig. 3C; P<0.01). These combined data indicate that in the absence of *dimm*, there is a reduction in levels of both secretory peptide mRNAs and secretory peptides.

To examine further the effect of disruptions in *CG8667* expression, we performed RNAi analysis and observed reduced levels of MM immunostaining in hatchling stage larvae (Fig. 2D). The reduction in MM immunostaining was comparable with the phenotype in null *dimm*$^{-/-}$ mutants (Fig. 2C). We obtained the same results using two additional antisera, PT2 and anti-LK (n=5 and n=6; data not shown). We also tested the ability of a *UAS-dimm::Myc* transgene to restore neuropeptide levels in *dimm*$^{-/-}$ animals. We used the *c127-Gal4* line to drive *dimm::Myc* expression in a small set of ventral CNS neurons, which included the 14 LK-positive cells in abdominal neuromeres (Fig. 4A). Expression of *dimm::Myc* selectively restored normal levels of LK immunostaining in *Rev8/Rev4* animals (n=19; Fig. 4C), but not in the absence of the *Gal4* driver (n=17; Fig. 4B). The rescue displayed cell specificity: the FMRF-positive MP2 neurons did not express *UAS-GFP* by *c127-Gal4*, and they were not rescued (n=10; data not shown). Together, these results support the hypothesis that *dimm* is the *Drosophila Mist1* ortholog, *CG8667*.

We performed a gain-of-function analysis by driving *UAS-dimm::myc* in an otherwise wild-type background. When misexpressed using a pan-neuronal *elav-GAL4* driver, most embryos died (data not shown). This suggested that the effects of *dimm* on shaping neuronal properties can be widespread. To permit a more restricted analysis, we used *ap-Gal4* (Fig. 4E-G), a *P{Gal4}* reporter inserted in the *apterous* (*ap*) gene (O'Keefe et al., 1998). When overexpressed in a subset of brain neurons, *dimm* increased the brightness of LK immunostaining in the cell body and processes of the LK-positive Br1 neuron (Fig. 3F,G). *dimm* overexpression did not produce widespread LK misexpression, but it reproducibly increased the number of LK-positive neurons from one (in animals lacking the *ap-Gal4* element, n=18 hemispheres) to two (n=22 hemispheres). The additional LK-positive neuron was always adjacent to the normal one. Thus, *dimm* can alter the properties of normal neuroendocrine cells, and it can affect the number of cells displaying a neuroendocrine phenotype.

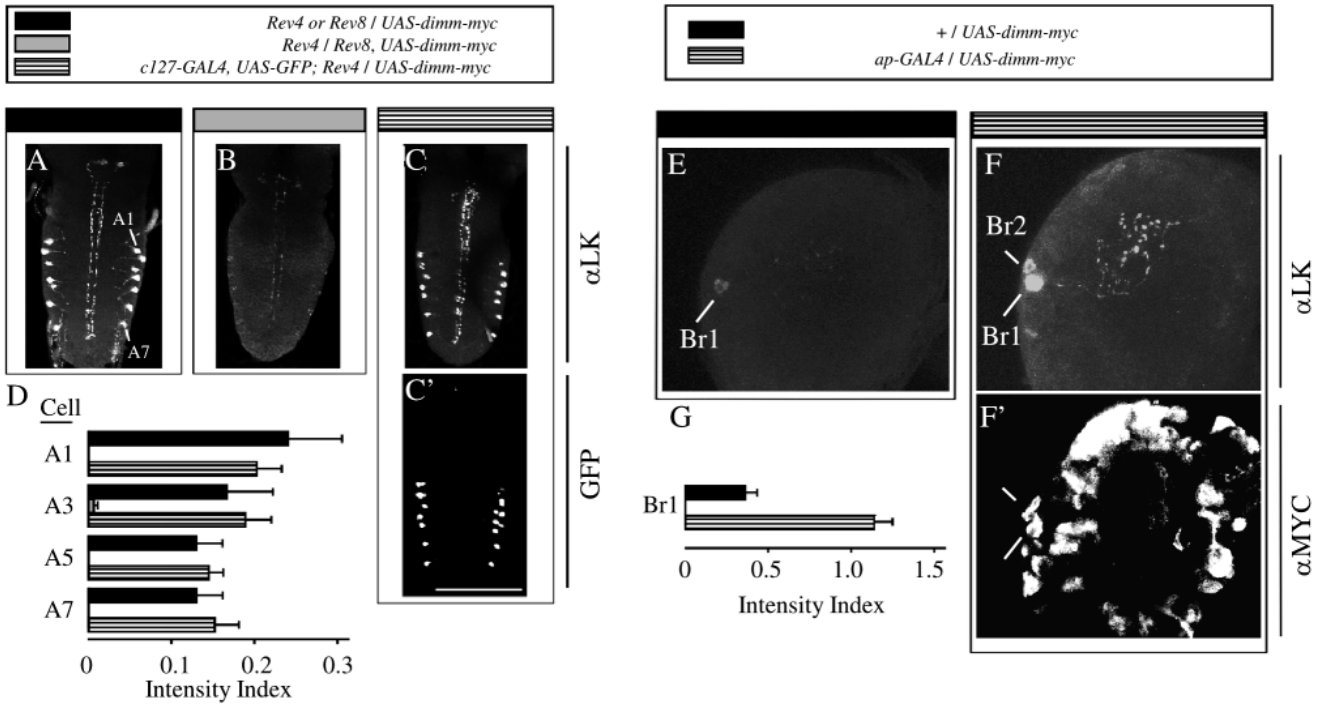

Fig. 4. Expression of wild-type *CG8667* restores neuropeptide levels in *dimm* mutants (left) and increases normal neuropeptide levels in wild-type animals (right). (A) LK immunostaining of the A1-A7 neurons in the ventral nerve cord in animals heterozygous for the *Rev8* or *Rev4* deficiencies. The *P{UAS-dimm::Myc}* transgene, which contains the entire predicted *CG8667* ORF, was present on the *Rev8* chromosome. (B) Markedly reduced LK immunostaining in *dimm*$^{-/-}$ (*Rev8*/*Rev4*) animals. (C) Staining levels in A1-A7 were restored to normal in *Rev8*/*Rev4* animals by inclusion of the *c127-Gal4* element. The A1-7 LK-positive neurons were all GFP positive at this stage (C′). (D) Mean pixel intensity (intensity index) for four pairs of LK-positive neurons in the three genotypes (NS, heterozygous versus rescue; P<0.01, homozygous versus rescue). (E) LK immunostaining of the Br1 neuron in the lateral brain of an animal wild type for *dimm* and containing one copy of the *UAS-dimm::myc* transgene. (F) LK-immunostaining in Br1 (soma and arbor) is markedly increased, and a neighboring neuron Br2 becomes LK positive, when *UAS-dimm-Myc* is driven by *ap-GAL4*. Br1 was identified based on the retained shape of its axonal arbor. (F′) Anti-Myc immunostaining of the specimen in F reveals that Br1 and Br2 neuron are both *ap-GAL4* positive. Scale bar, 50 μm in C; 20 μm in F. (G) Mean pixel intensity (intensity index) for the Br1 LK-positive neuron in the two genotypes (P<0.001).

CG8667 is specifically expressed in peptidergic neurons and endocrine cells

CG8667 mRNAs were ubiquitous in pre-cellular blastoderm embryos (Moore et al., 2000; data not shown) and later were expressed in the developing nervous system (Moore et al., 2000). Presumed zygotic *CG8667* expression was first visible as nascent transcripts scattered throughout the CNS in stage 12 embryos. Cytoplasmic *CG8667* hybridization was visible in many of these cells beginning around stage 14 (Fig. 5A), was strong by stage 16 (Fig. 5B) and persisted in stage 17 embryos (Fig. 5C) and in hatchling larvae less than 24 hour old (Fig. 5G).

The pattern of CNS *CG8667* in situ hybridization resembled the *c929* reporter pattern (Fig. 5A-C,G). Based on their positions and morphologies, more than 12 separate types of *CG8667*-expressing neurons were putatively identified as *c929* positive. These included dorsal chain neurons (e.g. d3-d5), T1-3v, LP1, MP1, MP2, SP1, T1-3vb and VA, as well as several bilateral clusters of neurons: large, midline protocerebral brain cells (MC), lateral protocerebral brain cells (LC), ventral subesophageal neurons (SE) and lateral abdominal neurons (neuromeres N1, N4 and N5).

We also observed expression of the *c929* reporter and *CG8667* in strikingly similar patterns in peripheral tissues (Fig. 5). These sites included the LBD neurons and several endocrine tissues: intrinsic cells of the corpora cardiaca, Inka cells and a few midgut cells. Numerically, all peripheral cell types were equally represented, except that there were fewer *CG8667*-expressing gut cells in embryos than *c929*-positive gut cells of larvae. *CG8667* was not expressed in any other location, except for a few unidentified non-CNS cells scattered throughout the anterior and lateral regions (stages 12-15). Thus, in CNS, PNS and endocrine tissues, expression of the *c929* reporter closely mirrored *CG8667* expression. These expression analyses support the genetic mapping, genetic identification and RNAi data. Thus, from this point onwards we refer to *CG8667* as *dimmed*.

dimm mutant cells survive and arborize normally

We next determined whether secretory cells survived and differentiated in *dimm*$^{-/-}$ mutant animals. In larvae homozygous for the null allele, *Rev4*, some of the affected cells displayed low residual immunostaining for secretory proteins (e.g. Fig. 2B,C). Thus, some *dimm*-expressing cells survived in mutant larvae and were at least

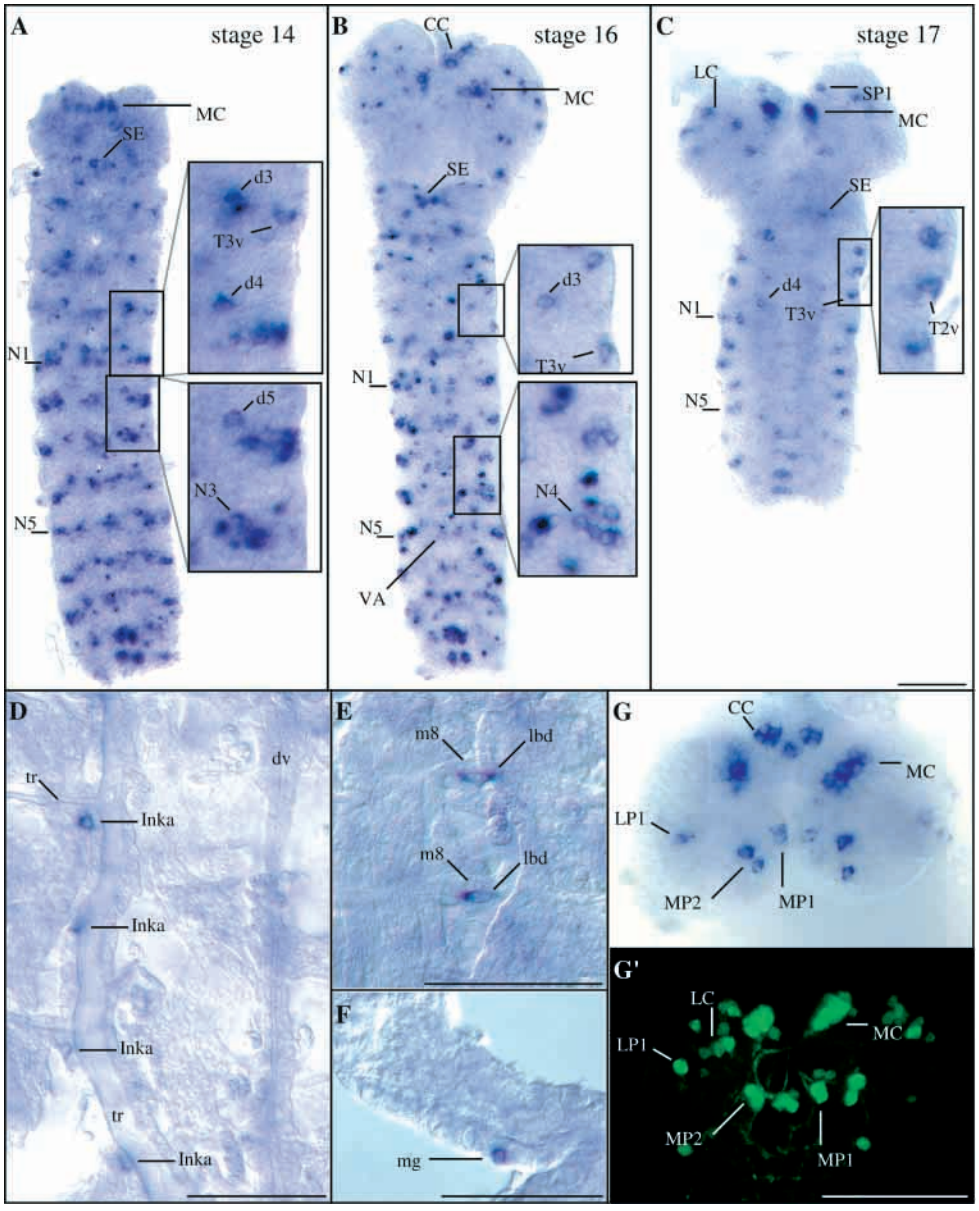

Fig. 5. *dimm* mRNA is expressed in a *c929*-like pattern of differentiating and post-embryonic peptidergic cells. (A-C) Photomontages of *dimm* in situ hybridization in embryonic CNS (A, stage 14; B, stage 16; C, stage 17). (D-F) Photomontages of *dimm* in situ hybridization in the Inka cells (D, stage 17), the peptidergic LBD neurons (LBD), which are adjacent to muscle 8 (m8) (E, stage 15), and a gut cell (mg) at the base of the anterior region of the midgut (F, stage 17). The ventral midline (D-E) is towards the left and anterior is upwards. dv, dorsal vessel; tr, tracheae. (G) Matching patterns of *dimm* expression revealed by in situ hybridization (G, photomontage) and the *c929* reporter (G′, confocal image) in the brain lobes of hatchling (first instar) larvae. The LC cells are present but out of focus in G (compare with C). The intrinsic cells of the corpora cardiaca (CC) were removed during dissection of the brain in G′. Scale bars: 50 μm in A-G; 20 μm in insets in A-C.

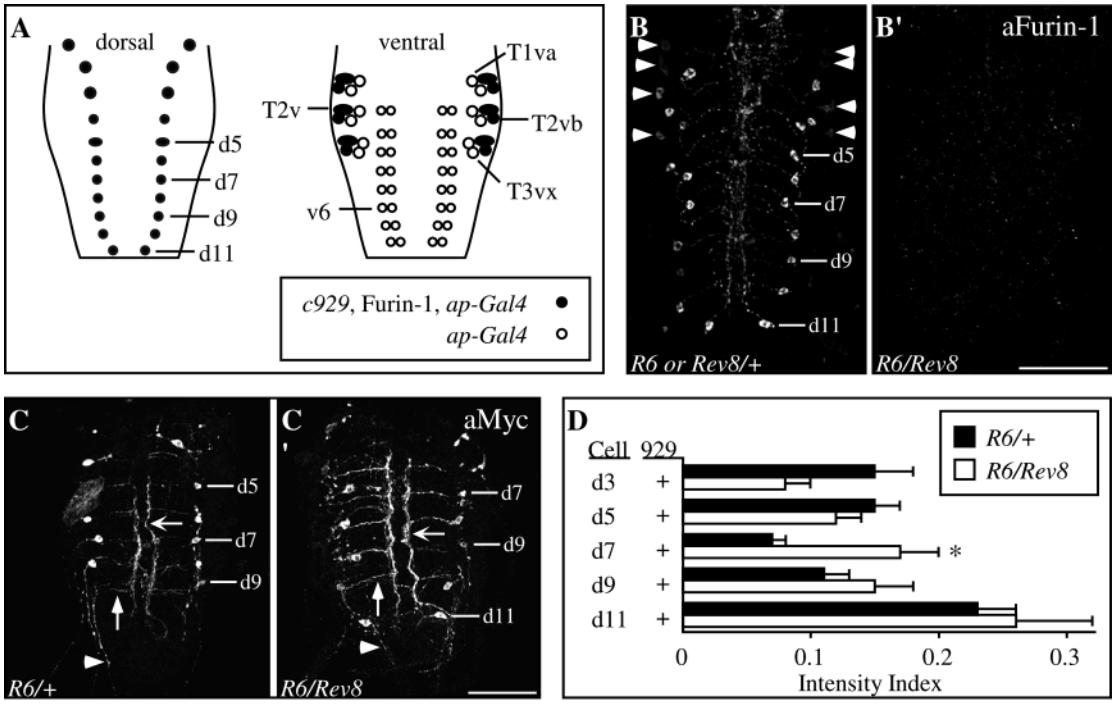

Fig. 6. *dimm*$^{-/-}$ mutant neurons differentiate, survive, and express non-secretory proteins at normal levels. (A) Thirty-four neurons (black circles) in the ventral nerve cord that co-express the *c929* reporter, Furin 1 and *ap-Gal4* (*ap*^{Gal4}). Additional ventral neurons (white circles) express *ap-Gal4* but do not express the other two markers. (B) The *dimm* mutant phenotype for the 34 Furin 1 neurons. Reduction in Furin 1 immunostaining in the CNS of a third instar *dimm*$^{-/-}$ (*R6/Rev8*) larva (B′), compared with a *dimm*$^{+/-}$ (*R6* or *Rev8/+*) sibling control (B) (n>50). Arrowheads indicate Tv and Tvb neurons. (C) Ectopic expression of the non-secretory fusion protein tau::Myc in the 34 Furin 1-positive neurons. In *dimm*$^{-/-}$ mutant CNS (third instar; *R6, ap-Gal4/Rev8; UAS-tau::Myc/+*), all 34 Furin 1 neurons displayed anti-Myc immunostaining (C′) that was comparable with that in the *dimm*$^{+/-}$ sibling control (C; *R6, ap-Gal4/+; UAS-tau::Myc/+*). In both genotypes, each of the dorsal chain neurons (d1-d11) displayed projections that extended toward the midline (vertical arrows) and then ran longitudinally (horizontal arrows). We also observed normal immunostained projections in each abdominal nerve (arrowheads). (D) Mean pixel intensity (intensity index) for soma Furin 1 immunostaining in five pairs of dorsal chain neurons in seven *dimm*$^{+/-}$ and 13 *dimm*$^{-/-}$ CNSs. *P<0.05. Scale bars: 50 μm.

partially differentiated. Others displayed a complete loss of peptide immunostaining, and their status was unclear.

In order to determine the fates of the latter cells, we used *Gal4/UAS* mosaics to express ectopic, non-secretory proteins in *dimm* mutant neurons. We studied 34 CNS neurons that co-expressed three different markers: the *c929* reporter, the putative peptide biosynthetic enzyme Furin 1, and *ap-Gal4* (Fig. 6A; P.H.T. and M. Han, unpublished). In *dimm*$^{-/-}$ larval CNS, all 34 neurons displayed strongly reduced, and often undetectable, immunostaining for Furin 1 (Fig. 6B). Using *ap-Gal4* to drive heterologous expression of a tau::Myc fusion protein, we found that all 34 of these neurons were present and displayed normal morphology in the *dimm*$^{-/-}$ larvae (Fig. 6C). In addition, the intensity of anti-Myc immunostaining was not affected (Fig. 6D). We obtained identical results using green fluorescent protein (GFP) to mark the cells (n=6; data not shown). Thus, *dimm* mutant neurons displayed multiple differentiated features and synthesized non-secretory proteins at normal levels throughout larval development.

We also examined the effects of *dimm* on the terminal arbor of the LK-positive neurons. These cells displayed reduced soma LK immunostaining in *dimm*$^{-/-}$ CNS (Fig. 4B). Each neuron had a single efferent axon that projected across the posterior muscle 8 surface and terminated dorsally near a tracheal branch. In third instar *dimm*$^{-/-}$ larvae, these axons also displayed reduced LK immunostaining. However, a sufficient number of immunoreactive boutons remained to indicate a normal axonal expanse (see Fig. S1 at http://dev.biologists.org/supplemental/). Thus, the effects of *dimm* on this LK neuron appear limited to expression of the transmitter phenotype.

dimm affects levels of proteins destined for both regulated and constitutive secretion

Our earlier measures of the *dimmed* phenotype were restricted to analysis of proteins abundant in the regulated secretory pathway. We also tested for an effect of *dimm* on constitutively secreted proteins. With *ap-Gal4*, we directed expression of a CD8::GFP fusion protein (*UAS-CD8::GFP*) to a subset of *dimm*-expressing neurons. CD8 is an integral membrane protein that is targeted to the plasma membrane in *Drosophila* cells (Zito et al., 1997). In *dimm*$^{-/-}$ mutant larvae, all 34 *ap-Gal4* (Furin-1) neurons expressed CD8::GFP and displayed normal neuritic projections. However, CD8::GFP levels were significantly lower in *c929*-positive neurons in the *dimm*$^{-/-}$ background (see Fig. S2 at http://dev.biologists.org/supplemental/). This effect was more subtle than the effects on levels of regulated secretory proteins. However, it suggests that *dimm* influences both regulated and constitutive secretory activity in neuroendocrine cells.

dimm regulates multiple elements of the secretory pathway

Because *ap*-dependent expression of transgenes was unaffected by *dimm* (Fig. 6C), we were able to uncouple neuropeptide transcription from potential effects of *dimm* on secretory activity. Thus, when *ap-Gal4* drove ectopic expression of the *pdf* neuropeptide gene, ectopic *pdf* mRNA levels were

unaffected in *dimm*$^{-/-}$ larvae (Fig. 7A,B). By contrast, ectopic PDF protein levels were severely reduced. We performed immunostaining for two peptide epitopes of the proPDF precursor (Renn et al., 1999): PAP (Fig. 7C,F) and PDF (*n*=20; data not shown). All 34 (*c929*-positive) neurons displayed severely reduced immunostaining for both PDF-related epitopes. Additional ventral abdominal neurons served as internal controls. These included 44 neurons that also displayed ectopic *pdf* expression driven by *ap-Gal4*, and a set of approximately eight native *pdf* neurons (not *ap*-positive). All of the internal control cells were *c929* negative, and PAP/PDF immunostaining in these neurons was unaffected in *dimm*$^{-/-}$ larvae (Fig. 7C-F). Thus, *dimm* was required within *c929*-positive neurons for the maintenance of ectopic PDF neuropeptide levels, but not of ectopic *pdf* mRNA.

DISCUSSION

Dimm is the first example of a dedicated pro-secretory factor. Dimm is necessary to confer neuroendocrine features onto peptidergic neurons that, in its absence, survive with normal neuronal properties. In addition, Dimm overexpression produces supra-normal levels of neuropeptide expression in peptidergic neurons and the appearance of additional cells with neuroendocrine features. From this genetic analysis, we suggest that neuroendocrine cell differentiation includes two interrelated, but separate sets of instructions. The first specifies the identity of the neuropeptide(s) or peptide hormone(s) to be expressed, while the second, which involves Dimm, specifies the level of regulated secretory activity.

The bHLH domain of the predicted Dimm protein showed the highest degree of sequence identity with the mouse, rat and human Mist1 proteins. These proteins may be orthologs (Moore et al., 2000). Interestingly, mouse Mist1 is present in many adult peripheral tissues, but within these tissues it is found only in serous exocrine cells (Pin et al., 2000). The restriction of mouse Mist1 expression to dedicated secretory cells suggests that *dimm* and mouse Mist1 may both control levels of secretory activity, and so may perform evolutionarily conserved functions. Other members of the Atonal family are expressed in both differentiating and terminally differentiated cells (e.g. NeuroD) (Morrow et al., 1999). Several mammalian Atonal family bHLH proteins have previously been implicated in earlier stages of endocrine cell

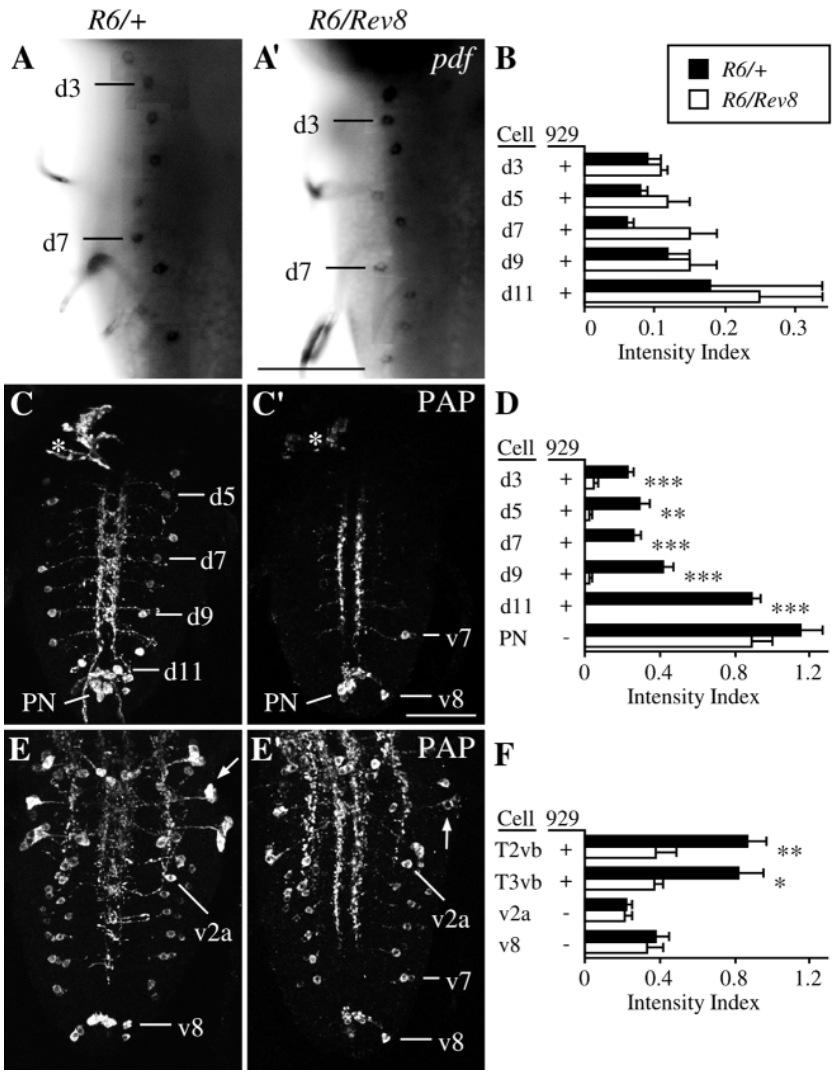

Fig. 7. *dimm* controls levels of ectopic neuropeptide (proPDF) but not levels of ectopic *pro-pdf* mRNA. (A) Brightfield photomontages of *pdf* mRNA in situ hybridization in the dorsal chain neurons of *dimm*$^{+/-}$ (A; *R6, ap-Gal4/+; UAS-pdf/+*) and *dimm*$^{-/-}$ (A′; *R6, ap-Gal4/Rev8; UAS-pdf/+*) third instar stage CNS. Heterologous expression of the *pdf* neuropeptide gene, which encodes the PAP neuropeptide, was directed to these neurons using *UAS-pdf* (Renn et al., 1999) and *ap-GAL4*. (B) Mean pixel intensity (intensity index) for *pdf* mRNA in situ hybridization in the somata of selected pairs of *c929*-positive dorsal neurons (*dimm*$^{+/-}$, *n*=11-12; *dimm*$^{-/-}$, *n*=8-9). (C) Confocal *z*-series images of dorsal PAP (proPDF) immunostaining in the CNS from *dimm*$^{-/+}$ (C) and *dimm*$^{-/-}$ (C′) third instar stage larvae. Reduced staining (C′) was observed in the dorsal chain neurons (d1-11) and the dorsal neurohemal organs (asterisks), which contain the neuroendocrine terminals of the Tv neuron (Benveniste and Taghert, 1999). Note that staining levels in *c929*-negative cells were unaffected: these included PN (natively *pdf*-positive), and v7 and v8 (ectopic, *ap-Gal4*-dependent expression). (D) Mean pixel intensity (intensity index) for PAP immunostaining in the somata of selected pairs of dorsal neurons and in the PN neurons (*dimm*$^{+/-}$, *n*=6; *dimm*$^{-/-}$, *n*=5). (E) Confocal *z*-series images of ventral PAP immunostaining in T2v (arrows) and in the ventral chain neurons, including v2a and v8, of a *dimm*$^{-/+}$ third instar stage CNS (E; same CNS as C) and a *dimm*$^{-/-}$ CNS (E′; same CNS as C′). The Tv neurons (arrows) express the *c929* reporter gene (Fig. 1C,E) and display the *dimm* mutant phenotype. By contrast, the ventral chain neurons do not express the reporter gene (data not shown), and they do not display the *dimm* mutant phenotype. (F) Mean pixel intensity (intensity index) for PAP immunostaining in the somata of selected pairs of ventral neurons (*dimm*$^{+/-}$, *n*=6; *dimm*$^{-/-}$, *n*=5). The brightest cell in each Tv cluster was assumed to be Tvb (P.H.T. and M. Han, unpublished). **P*<0.05, ***P*<0.01, ****P*<0.001. Scale bars: 50 μm.

development, including cell lineage commitment (e.g. Yang et al., 2001) and endocrine cell differentiation (Sheng and Westphal, 1999).

In *Drosophila*, *dimm* performs a novel, pro-secretory function in a diverse population of peptidergic CNS and PNS neurons and endocrine cells. In its absence, peptidergic cells complete many aspects of their differentiation – some express low levels of appropriate peptide transmitters. However, they uniformly fail to display normal amplified levels of secretory activity, which is a characteristic and fundamental property of peptidergic secretory cells (Arvan and Castle, 1998). How such cells acquire and maintain this capacity is largely unknown. We have shown that it is under the control of specific genetic mechanisms, as revealed by animals deficient in expression of the *dimm* gene. These experiments indicate that *dimm* plays a fundamental role in the differentiation of neuroendocrine lineages.

We propose a working model in which Dimm directly regulates transcription of genes required for production of a neuroendocrine phenotype – genes encoding neuropeptides, peptide hormones and peptide biosynthetic enzymes. Consistent with this model, we found that *dimm* reduces the normally high levels of *Fmrf* neuropeptide mRNA in specific neuroendocrine cells. In addition, Dimm also may regulate expression of proteins (e.g. transcription factors, or structural or regulative proteins of dense core granules) that are important for the function and amplification of the secretory pathway [e.g., as suggested by Kim et al. (Kim et al., 2001)]. Dimm functions after cell fate determination and during the early differentiation of these neurons – in *dimm* mutants, affected peptidergic neurons are present, arborize normally and often express low levels of appropriate neuropeptides.

Some secretory proteins form dense aggregations (‘progranules’) in the trans-Golgi network prior to their uptake into immature secretory granules. Similarly, condensation of secretory proteins during subsequent granule maturation may be required for their retention in maturing granules (Arvan and Castle, 1998). Therefore, direct reductions in the levels of a small number of target secretory proteins in *dimm* mutant cells may lead to a secondary disruption in aggregation or condensation of other proteins. In turn, these effects could lead to loss of most secretory proteins by mis-routing and degradation. This may account for our observation that secretory peptide levels could be reduced in a *dimm* mutant background, despite the artificial elevation of the cognate secretory peptide mRNA (Fig. 7).

Does *dimm* also regulate the constitutive secretory pathway? Although constitutive secretion was quantitatively affected by loss of *dimm* function, mutant neurons maintained their normal cellular morphology. These observations suggest that Dimm has only moderate effects on the constitutive secretory pathway. Given the physical interactions between cargoes destined for the regulated and constitutive pathways (Arvan and Castle, 1998), the reduction in constitutive secretion may reflect an indirect effect of disruptions in the regulated pathway.

We favor the view that during development and maturity, *dimm* expression is a crucial determinant of high secretory protein expression in neuroendocrine cells. This hypothesis was supported by the gain-of-function analysis. Overexpression of *dimm* in a wild-type background produced higher levels of LK expression in the normally LK-positive Br1 neuroendocrine neuron. It also increased the number of cells that display the specific LK neuroendocrine phenotype, but only within the immediate proximity of Br1. In this case, *dimm* overexpression was driven by a promoter (*ap-GAL4*) that is only expressed in postmitotic neurons. Therefore, it appears likely that the additional LK immunoreactive neurons represent cells that normally express LK but at levels that are too low to be detected. In addition, the limited number of ectopic leukokinin cells is likely a function of the specific *GAL4* driver used (*ap* is only expressed in a subset of cells), and the marker assayed (LK is only expressed in ~20 out of 10,000 neurons). Although the complete extent of the effects of *dimm*, when overexpressed, is not yet known it is likely to be large, as *UAS-dimm* produces large-scale embryonic lethality when driven by the pan-neuronal *elav-GAL4* (D. P., unpublished).

Accordingly, we propose that *dimm* promotes diverse neuroendocrine cell fates in different cellular locales, depending on local cellular context and identity. We observed *dimm* expression soon after cells cease dividing, and in its absence, most of these cells were deficient in ‘transmitter expression’. Thus, Dimm appears to function like NeuroD proteins, which are also members of the Atonal family and which act as cell differentiation factors (Hassan and Bellen, 2000).

Analysis within the identified, neuroendocrine Tv neurons may be especially informative to reveal further details of the mechanisms of *dimm* action. Four regulatory factors have now been defined that affect FMRF neuropeptide levels in Tv neurons. Loss-of-function *ap* (Benveniste et al., 1998), *Chip* (Van Meyel et al., 2000) and *dimm* (this report) alleles all decrease Tv-specific FMRF expression, but do not influence Tv survival or morphology. Likewise, the *squeeze* (*sqz*) gene helps regulate Tv-specific FMRF levels (S. Thor, personal communication). Within Tv neurons, *ap*, *Chip*, *dimm* and *sqz* may function in a linear pathway to regulate *Fmrf* gene expression, akin to the sequential actions of the bHLH protein MASH1 and the Phox2 homeoproteins in neurons of the locus coeruleus (Pattyn et al., 2000). Alternatively, they may work in parallel fashion, akin to the synergistic interactions between the bHLH NeuroD1 and the LIM homeoproteins Lmx1.1 and Lmx1.2 to control insulin expression (Ohneda et al., 2000). As a first step, we have shown that *ap* promoter function is independent of *dimm*. Further work will permit description of the molecular pathways controlling qualitative and quantitative aspects of neuroendocrine cell differentiation in vivo.

We thank Weihua Li and Aloka Amarakone for technical assistance, and Hans Agricola, Doug Allan, Hugo Bellen, Gabrielle Boulianne, Adelaide Carpenter, Heinrich Dircksen, Chris Doe, Dan Eberl, John Ewer, Jeff Hall, Mike Horner, Yuh-Nung Jan, Iris Lindberg, Dick Nässel, Jae Park, Anton Roebroek, Steve Scholnick, Amy Sheehan, John Thomas, Stephan Thor, Carl Thummel, Jan Veenstra, Klaude Weiss and Andrew Zelhof for information, DNA, antibodies or fly stocks. We thank Lou Muglia, Jim Skeath and Stefan Thor for comments on the manuscript, the Bloomington Stock Center for fly stocks, and the BDGP for DNA sequence. This work was supported by an American Cancer Society Postdoctoral Fellowship PF4212 (R.S.H.) and by a grant NS21749 from the NIH (P.H.T.).

REFERENCES

Acampora, D., Postiglione, M. P., Avantaggiato, V., di Bonito, M., Vaccarino, F. M., Michaud, J. and Simeone, A. (1999). Progressive

impairment of developing neuroendocrine cell lineages in the hypothalamus of mice lacking the *Orthopedia* gene. *Genes Dev*. **13**, 2787-2800.

Arvan, P. and Castle, D. (1998). Sorting and storage during secretory granule biogenesis: looking backward and looking forward. *Biochem. J.* **332**, 593-610.

Benveniste, R. J. and Taghert, P. H. (1999). Cell type-specific regulatory sequences control expression of the *Drosophila FMRF-NH$_2$* neuropeptide gene. *J. Neurobiol.* **38**, 507-520.

Benveniste, R. J., Thor, S., Thomas, J. B. and Taghert, P. H. (1998). Cell type-specific regulation of the *Drosophila FMRF-NH$_2$* neuropeptide gene by Apterous, a LIM homeodomain transcription factor. *Development* **125**, 4757-4765.

Blake-Bruzzini, K. M., Borke, R. C., Anders, J. J. and Potts, J. D. (1997). Calcitonin gene-related peptide and *alpha-CGRP* mRNA expression in cranial motoneurons after hypoglossal nerve injury during postnatal development. *J. Neurocytol.* **26**, 163-179.

Burbach, J. H. P., Luckman, S. M., Murphy, D. and Gainer, H. (2001). Gene regulation in the magnocellular hypothalmo-neurohypophyseal system. *Physiol. Rev*. **81**, 1197-1267.

Clemens, J. C., Worby, C. A., Simonson-Leff, N., Muda, M., Maehama, T., Hemmings, B. A. and Dixon, J. E. (2000). Use of double-stranded RNA interference in *Drosophila* cell lines to dissect signal transduction pathways. *Proc. Natl. Acad. Sci. USA* **97**, 6499-6503.

Chin, A., Reynolds, E. and Scheller, R. H. (1990). Organization and expression of the *Drosophila FMRFamide-related* prohormone gene. *DNA Cell Biol*. **9**, 263-271.

De Bie, I., Savaria, D., Roebroek, A. J., Day, R., Lazure, C., van de Ven, W. J. and Seidah, N. G. (1995). Processing specificity and biosynthesis of the *Drosophila melanogaster* convertases dfurin1, dfurin1-CRR, dfurin1-X, and dfurin2. *J. Biol. Chem*. **270**, 1020-1028.

Eipper, B. A., Stoffers, D. A. and Mains, R. E. (1993). Biosynthesis of neuropeptides: alpha-amidation. *Annu. Rev. Neurosci*. **15**, 57-85.

Ewer, J. and Truman, J. W. (1996). Increases in cyclic 3′,5′-guanosine monophosphate (cGMP) occur at ecdysis in an evolutionarily conserved crustacean cardioactive peptide-immunoreactive insect neuronal network. *J. Comp. Neurol.* **370**, 330-341.

FlyBase (1999). The FlyBase database of the *Drosophila* genome projects and community literature. The FlyBase Consortium. *Nucleic Acids Res*. **27**, 85-88.

Hall, Z. W. and Sanes, J. R. (1993). Synaptic structure and development: the neuromuscular junction. *Cell Suppl.* **72**, 99-121.

Hassan, B. A. and Bellen, H. J. (2000). Doing the MATH: is the mouse a good model for fly development? *Genes Dev*. **14**, 1852-1865.

Herman, J. P., Schaefer, M. K., Watson, S. J. and Sherman, T. J. (1991). In situ hybridization analysis of arginine vasopressin gene transcription using intron-specific probes. *Mol. Endocrinol*. **5,** 1447-1456.

Hewes, R. S. and Taghert, P. H. (2001). Neuropeptides and neuropeptide receptors in the *Drosophila melanogaster* genome. *Genome Res*. **11**, 1126-1142.

Hewes, R. S., Schaefer, A. and Taghert, P. H. (2000). The *cryptocephal* gene (ATF4) encodes multiple basic-leucine zipper proteins controlling molting and metamorphosis in *Drosophila*. *Genetics* **155**, 1711-1723.

Hirsh, J. (1989). Molecular genetics of dopa decarboxylase and biogenic amines in *Drosophila*. *Dev. Genet.* **10**, 232-238.

Jiang, N., Kolhekar, A. S., Jacobs, P. S., Mains, R. E., Eipper, B. A. and Taghert, P. H. (2000). PHM is required for normal developmental transitions and for biosynthesis of secretory peptides in *Drosophila*. *Dev. Biol*. **226**, 118-136.

Kennerdell, J. R. and Carthew, R. W. (1998). Use of dsRNA-mediated genetic interference to demonstrate that *frizzled* and *frizzled 2* act in the Wingless pathway. *Cell* **95**, 1017-1026.

Kim, T., Tao-Cheng, J., Eiden, L. E. and Loh. Y. P. (2001). Chromogranin A, an 'On/Off' switch controlling dense-core secretory granule biogenesis. *Cell* **106**, 499-509.

Lindsley, D. L. and Zimm, G. G. (1992). *The genome of* Drosophila melanogaster. San Diego, CA: Academic Press.

Michaud, J. L., Rosenquist, T., May, N. R. and Fan, C. M. (1998). Development of neuroendocrine lineages requires the bHLH-PAS transcription factor SIM1. *Genes Dev*. **12**, 3264-3275.

Moore, A. W., Barbel, S., Jan, L. Y. and Jan, Y. N. (2000). A genome-wide survey of basic helix-loop-helix factors in *Drosophila*. *Proc. Natl. Acad. Sci. USA* **97**, 10436-10441.

Morrow, E. M., Furukawa, T., Lee, J. E. and Cepko, C. L. (1999). NeuroD regulates multiple functions in the developing neural retina in rodent. *Development* **126**, 23-36.

Nakai, S., Kawano, H., Yudate, T., Nishi, M., Kuno, J., Nagata, A., Jishage, K., Hamada, H., Fujii, H. and Kawamura, K. (1995). The POU domain transcription factor Brn-2 is required for the determination of specific neuronal lineages in the hypothalamus of the mouse. *Genes Dev*. **9**, 3109-3121.

Nässel, D. R. and Lundquist, C. T. (1991). Insect tachykinin-like peptide: distribution of leucokinin immunoreactive neurons in the cockroach and blowfly brains. *Neurosci. Lett*. **130**, 225-228.

O'Brien, M. A. and Taghert, P. H. (1998). A peritracheal neuropeptide system in insects: release of myomodulin-like peptides at ecdysis. *J. Exp. Biol.* **201**, 193-209.

O'Keefe, D. D., Thor, S. and Thomas, J. B. (1998). Function and specificity of LIM domains in *Drosophila* nervous system and wing development. *Development* **125**, 3915-3923.

Ohneda, K., Ee, H. and German, M. (2000). Regulation of insulin gene transcription. *Semin. Cell Dev. Biol*. **11**, 227-233.

Patel, N. H. (1996). In situ hybridization to whole mount *Drosophila* embryos. In *A Laboratory Guide to RNA* (ed. P. A. Krieg), pp. 357-370. New York: Wiley-Liss.

Pattyn, A., Goridis, C. and Brunet, J. F. (2000). Specification of the central noradrenergic phenotype by the homeobox gene Phox2b. *Mol. Cell. Neurosci.* **15**, 235-243.

Pin, C. L., Bonvissuto, A. C. and Konieczny, S. F. (2000). Mist1 expression is a common link among serous exocrine cells exhibiting regulated exocytosis. *Anat. Rec*. **259**, 157-167.

Pin, C. L., Lemercier, C. and Konieczny, S. F. (1999). Cloning of the murine *Mist1* gene and assignment to mouse chromosome band 5G2-5G3. *Cytogenet. Cell. Genet*. **86**, 219-222.

Renn, S. C., Park, J. H., Rosbash, M., Hall, J. C. and Taghert, P. H. (1999). A *pdf* neuropeptide gene mutation and ablation of PDF neurons each cause severe abnormalities of behavioral circadian rhythms in *Drosophila*. *Cell* **99**, 791-802.

Schneider, L. E., Sun, E. T., Garland, D. J. and Taghert, P. H. (1993). An immunocytochemical study of the FMRFamide neuropeptide gene products in Drosophila. *J. Comp. Neurol.* **337**, 446-460.

Scholnick, S. B., Caruso, P. A., Klemencic, J., Mastick, G. S., Mauro, C. and Rotenberg, M. (1991). Mutations within the *Ddc* promoter alter its neuron-specific pattern of expression. *Dev. Biol.* **146**, 423-437.

Schonemann, M. D., Ryan, A. K., McEvilly, R. J., O'Connell, S. M., Arias, C. A., Kalla, K. A., Li, P., Sawchenko, P. E. and Rosenfeld, M. G. (1995). Development and survival of the endocrine hypothalamus and posterior pituitary gland requires the neuronal POU domain factor Brn-2. *Genes Dev*. **9**, 3122-3135.

Sheng, H. Z. and Westphal, H. (1999). Early steps in pituitary organogenesis. *Trends Genet*. **15**, 236-240.

Streit, W. J., Dumouli, F. L., Raivich, G. and Kreutzberg, G. W. (1989). Calcitonin gene-related peptide increases in rat facial motoneurons after peripheral nerve transections. *Neurosci. Lett.* **101**, 143-148.

Taghert, P. H. (1999). FMRFamide neuropeptides and neuropeptide-associated enzymes in *Drosophila*. *Microsc. Res. Tech.* **45**, 80-95.

Tautz, D. and Pfeifle, C. (1989). A non-radioactive in situ hybridization method for the localization of specific RNAs in *Drosophila* embryos reveals translational control of the segmentation gene *hunchback*. *Chromosoma* **98**, 81-85.

van Meyel, D. J., O'Keefe, D. D., Thor, S., Jurata, L. W., Gill, G. N. and Thomas, J. B. (2000). Chip is an essential cofactor for apterous in the regulation of axon guidance in *Drosophila*. *Development* **127**, 1823-1831.

Veenstra, J. A. (1994). Isolation and structure of the *Drosophila corazonin* gene. *Biochem. Biophys. Res. Commun.* **204**, 292-296.

Yang, Q., Bermingham, N. A., Finegold, M. J. and Zoghbi, H. Y. (2001) Requirement of *Math1* for secretory cell lineage commitment in the mouse intestine. *Science* **294**, 2155-2158.

Yeh, E., Gustafson, K. and Boulianne, G. L. (1995). Green fluorescent protein as a vital marker and reporter of gene expression in *Drosophila*. *Proc. Natl. Acad. Sci. USA* **92**, 7036-7040.

Zito, K., Fetter, R. D., Goodman, C. S. and Isacoff, E. Y. (1997). Synaptic clustering of Fasciclin II and Shaker: essential targeting sequences and role of Dlg. *Neuron* **19**, 1007-1016.

Table S1. Neuropeptide staining of 39C4-D1 alleles

	Allele
Reduced neuropeptide levels	*dimm*^{KG02598}
	Df(2L)Rev4
	Df(2L)DS8
	Df(2L)Rev8
	*Df(2L)R6**
	Df(2L)R6
Normal neuropeptide levels	*crc*^{1}
	crc^{929}
	crc^{R1}*
	crc^{R2}
	Df(2L)TW1
	Sco
	Rev(KG02598)S2a

The phenotype of each allele was assessed either in homozygotes, in hemizygotes (in trans with a deficiency of 39C4-D1) or in both homozygotes and hemizygotes.

*Chromosomes outcrossed for at least seven generations.

Table S2. Complementation analysis of *dimm*^{KG02598}

dimm class	*crc* class	Allele	*n*	% Cy$^+$ expected
Severe hypomorph	+	*dimm*^{KG02598}	124	0‡
Severe hypomorph	+	*dimm*^{KG02598}§	120	0‡
Null	Null	*Df(2L)Rev4*	176	3‡
N.D.	Null	*Df(2L)DS8*	135	0‡
N.D.	Null	*Df(2L)DS5b*	148	0‡
Hypomorph	Null	*Df(2L)Rev8*	219	11‡
Hypomorph	Severe hypomorph	*Df(2L)R6*¶	120	0‡
Hypomorph	Severe hypomorph	*Df(2L)R6*	269	2‡
N.D.	Severe hypomorph	*crc*^{4351}	145	54‡
+	Severe hypomorph	*crc*^{1}	263	70‡
+	5′ hypomorph*	*crc*^{929}	247	120†
+	5′ hypomorph*	*crc*^{R1}¶	130	100
+	+	*Df(2L)TW1*	264	120
+	+	*Sco*	148	108
N.D.	N.D.	*Rev(KG02598)1*	141	132‡
N.D.	N.D.	*Rev(KG02598)13*	150	122

The female parents in each cross were *dimm*^{KG02598} (*dimm*^{KG02598} males were used for crosses with *crc*^{R1} and *Sco*). Two precise excisions of *KG02598*, *Rev(KG02598)1* and *Rev(KG02598)13* (females), were crossed to *Df(2L)Rev4* (males). The percentages of expected *Cy*$^+$ progeny were calculated from the number of *Cy*$^–$ siblings.

*Specific disruption of only the 5′ exons of *crc* (exons encoding *crc*-b transcript are intact) (Hewes et al., 2000).

†$P<0.05$ (χ^2 test)

‡$P<0.001$ (χ^2 test)

§Chromosomes outcrossed for eight generations

¶Chromosomes outcrossed for at least seven generations.

N.D., not done.